TÉCNICO LISBOA

Master Dissertation in Biomedical Technologies

Extended Abstract

Advances in Duchenne Muscular Dystrophy gene therapy: Test of BSA nanocapsules for nucleic acid delivery

Diana Margarida de Almeida Arteiro

Examination Committee

Chairperson: Professor Raúl Daniel Lavado Carneiro Martins

Supervisor: Professor Célia da Conceição Vicente Carvalho

Vowel: Professor Evguenia Pavlovna Bekman

Abstract: Duchenne Muscular Dystrophy (DMD) is an X-linked recessive disease caused mainly by frame-shifting or nonsense mutations in the gene of dystrophin, a protein essential for maintaining muscle cell membrane integrity. It was shown in DMD patients a complete absence of dystrophin in their muscles. Antisense-mediated exon skipping can restore the open reading frame and allow synthesis of a partially functional dystrophin in cultured DMD patient derived cells. Currently, antisense oligonucleotides (AONs) mediated exon skipping is a molecular therapeutic approach under development for DMD because it is expected that DMD patients would improve considerably if their muscle cells were able to produce some dystrophin even if it is at low level and even besides it is partially truncated, but functional.

Splicing modulation therapy, with AONs directed to induce exon skipping, to correct the production of dystrophin is under clinical trials but with limited results. AONs mediated human therapy still presents several barriers needed to be overcome: some related to pharmacokinetics, elimination/accumulation in the body, targeted delivery, and the low capacity to cross the plasma membrane unaided.

Nanoparticles have been explored as carriers to several therapeutic entities, presenting advantages such as tissue directed delivery, protection from degradation, improvement of dose efficiency and decrease of harmful side effects. Recent studies show a significantly improvement in nucleic acids delivery when associated to nanoparticles after IV administration in experimental animals.

Here we tested a new chemistry of modified AONs to treat a DMD mouse model, MDX52, by splice modulation gene therapy directed to induce skipping of exon 51 and therefore restore the reading frame and the production of the protein dystrophin in muscles. Regarding the suboptimal results, we hypothesized that therapeutic DNA molecules would have an increased uptake on target tissues, and subsequent correction of the phenotype, if the therapeutic nucleic acid was encapsulated on nanoparticles before being administered.

In order to first test the effect of encapsulation on nucleic acid in *in vivo* delivery we encapsulated a reporter plasmid pEGFP-NLS in BSA nanoparticles for IV administration on an animal model. The goal of this project was to evaluate the efficiency of gene delivery after systemic administration of the nanoparticles on experimental animals. The level of EGFP-NLS protein expression was accessed on target organs of injected animals by immunohistochemical analysis and by flow cytometry of dispersed cells from liver and lung. The study was complemented with an *in vitro* evaluation and characterization of the nanoparticles. Further studies will be needed to improve the development of this class of nanoparticles as carriers of nucleic acids for controlled delivery.

Key-words: Duchenne Muscular Dystrophy; gene therapy; exon skipping; *mdx52*; LNA-AON; controlled delivery systems; BSA nanoparticles; immunohistochemical analysis, fluorescent microscopy, flow cytometry.

1. Introduction

Duchenne Muscular Dystrophy (DMD) is the most common muscular dystrophy: it has an incidence of one in 4700 male live births in Canada (Nova Scotia) (Dooley et al, 2010). In most of the cases, Duchenne Muscular Dystrophy occurs due to frame-shifting deletions or nonsense mutations in the *DMD* gene encoding the dystrophin protein. Another related disorder that occur because of mutations in the *DMD* gene is Becker Muscular Dystrophy (BMD) with an incidence of 18450 live male births in northern England (Bushby et al, 1991). In DMD the gene mutations lead to complete absence of functional protein while in BMD a partially functional dystrophin protein is typically produced, leading to an attenuated clinical course and attenuated muscle pathologic abnormality (Wein et al, 2015). It is expected that DMD patients improve considerably if their muscle cells were able to produce some dystrophin protein, even if it is low and with a truncated part of the inner region, but functional.

No effective treatment exists for DMD. Although there are pharmacological strategies, such as administration of corticosteroids that treats inflammation and are able to delay symptoms by tackling the secondary effects of the disease, many are only partially effective because thy treat just one aspect of the pathogenesis and they also may be toxic in longer term. Antisense oligonucleotides (AONs) mediated exon skipping is a molecular therapeutic approach under development for DMD. In *mdx52* mouse model (containing mutation of exon 52), systemic delivery of AON recognizing exon 51 has shown proof of concept (Aoki et al, 2010).
AONs should be efficiently delivered into tissues and cells in order to reach their target and carry out their functions. However, several major obstacles, namely optimization of nontoxic effective doses, improvement of the delivery systems, distribution to all affected tissues, achievement of a sustainable therapeutic effect and development of an administration strategy suitable for lifelong treatment, still remain to be overcome. Nucleases are enzymes present at the surface mucosal and in the blood stream which are capable of degrading nucleic acids. Many nucleic acid carriers (liposomes, polymers and peptides) have been proposed to help nucleic acids to overcome those obstacles, but their clinical applicability is plagued by a lack of cell specificity and difficult in drug release. Recently, the focus turned to nanotechnology as a potential delivery system (Falzarano et al, 2014).

A class of materials that has emerged as being particularly promising to help nucleic acid therapeutic delivery is that of biocompatible protein nanocapsules, such albumin nanocapsules (Shimanovich et al, 2014). Albumin is non-toxic and degradable *in vivo*, so the nanoparticles generated by using it are easily adaptable to the human body. Levemir® and Abraxane® are two albumin-based drug delivery systems already approved and commercially available used to control high blood sugar in adults and children with *diabetes mellitus* type 1 and 2 and for the treatment of metastatic breast cancer, respectively (Elsadek et al, 2011). Recent studies in this field show a significantly improvement in dystrophin restoration in mice treated with nanoparticles encapsulating AON with respect to those treated with naked AON (Falzarano et al, 2014).

We hypothesized that therapeutic DNA molecules have an increased uptake on target tissues and subsequent expression of the encoding protein, if administrated in album nanoparticles.

1. Materials and Methods

1.1. LNA-AON

The short (16-mer) antisense DNA oligonucleotide targeting exon 51 in dystrophin transcript – 5’-AGGAAGATGGCATTTC-3’ – was purchased from Exiqon. It contains a fully phosphorothioate modified backbone and 60% LNA-modified nucleotides, with two LNA-modified nucleotides at the 3’-end and at the 5’-end. From previous (unpublished) experiments from our group, that compared different sequences and lengths of LNA-AONs, this LNA-AON was selected for this study because it presented the greatest capability of inducing skipping of exon 51 in myoblast derived human cell lines.

1.2. pEGFP-NLS amplification and purification

The reporter construct used in this study is pEGFP-NLS (Enhanced Green Fluorescent Protein). This reporter gene has a Nuclear Localization Signal (NLS) which is an amino acid sequence that allows signal the protein, for import into the cell nucleus so that fluorescent signal we see on the microscope has a specific pattern (Calado et al, 2000). The bacterial strain used for amplification was *Escherichia coli* DH5α cells (Invitrogen). *Escherichia coli* DH5α bacterial strain was transformed under Kanamycin (600 ng/µL) selection. Plasmid DNA from a 200mL bacterial culture was purified with Genopure Plasmid Midi Kit (Roche) according manufacturer instructions and further purified with UltraPure™ Phenol:Chloroform: Isoamyl Alcohol (Invitrogen, Cat. No. 15593-031, Lot. No. 2725C279).

1.3. BSA Nanocapsules

The reporter construct pEGFP-NLS was encapsulated on BSA nanocapsules by Gonçalo Bernarde's laboratory at the Department of Chemistry, University of Cambridge (Shimanovich et al, 2014). The stability of the BSA nanocapsules was assessed (after one month) by electrophoresis analysis. Naked plasmid, pEGFP-NLS/BSA nanocapsules and BSA nanocapsules (1µg each) were run for 60 minutes at 80 V on 1% agarose gel on TAE 1x buffer. The results were compared with a similar experiment after protein hydrolysis with proteinase K (Qiagen) for 10 minutes at 55ºC (according to manufacturer's instruction). The gel was photographed using gel documentation ChemiDoc™ XRS+ (Bio-Rad, model: XRS+) and digital images were obtained with Image Lab software (Bio-Rad). In order to confirm if the pDNA was indeed encapsulated, pEGFP-NLS/BSA nanocapsules were incubated with nucleic acid stain Hoechst 33342 (Invitrogen, Cat. No. H3570) for 10 minutes at RT and with Coomassie® Brilliant Blue R-250 (Bio-Rad, Cat. No. 161-0400), which stains specifically proteins, for 10 minutes at room temperature.

1.4. Cell culture

Human Embryonic Kidney 239 cells (HEK 293, ATCC® CRL-1573™) were maintained in complete medium consisting of in Dulbecco's Modified Eagle Medium (DMEM medium) (Gibco®, Cat. No. 41966-029) 10 % FBS (Fetal Bovine Serum, Gibco®, Ref. 10270-106) at a humidified atmosphere of 5 % CO_2 at 37ºC. For microscopy experiment cells were grown exceptionally on glass coverslips coated with poly-L-lysine (0.01% solution, Sigma-Aldrich®, Lot. RNBD4661).

In the transfection experiment, HEK 293 cells were plated in 6 well plates at a density of $2x10^5$ cells/well. Cells were transfected 1 day after being plated with Lipofectamine®3000 (Invitrogen, Ref. L3000-001, Lot. 1660194) according to manufacturer instructions. 0.067µg of plasmid DNA conjugated to 1µL of transfection reagent was added per well to 1.5mL of culture medium. Cells were incubated for 24 – 48 hours before subsequent analysis. The transfection of 0.013µg of plasmid DNA conjugated with 1µL of transfection reagent per well was also tested with good results. Negative control was done with no DNA.

In the transfection experiment with pEGFP-NLS/BSA nanocapsules, the equivalent of 0.067µg plasmid DNA, conjugated to 1µL of transfection reagent was added to each well. Negative control was the correspondent amount of BSA empty nanocapsules. Transfection with pEGFP-NLS/BSA nanocapsules was also tested eliminating the transfection reagent. In this case, in the same conditions 0.067µg of plasmid DNA with no transfection reagent was added per well. As a control naked pEGFP-NLS plasmid was used.

1.5. *In vivo* experiments

1.5.1. Animals

The exon 52-deficient X chromosome-linked muscular dystrophy mouse model (*mdx52*) was gently provided by Shin'ichi Takeda from National Center of Neurology and Psychiatry, Japan. These mice have been backcrossed to the C57BL/6J (WT) strain for more than eight generations (Aoki et al, 2012); WT C57BL/6J mice were purchased from Charles River. All animal care and experimental procedures were reviewed and ethically approved by the IMM Animal Ethics Committee and Portuguese competent authority for animal protection, Direcção Geral de Alimentação e Veterinária, Lisbon, Portugal.
To evaluate the capacity of the LNA-AON in restoring dystrophin production *in vivo*, 13-week-old *mdx52* mice were intravenously injected once in tail vein with 10mg/kg of LNA-AON (treated) or saline solution (control). The mice were sacrificed 11 weeks after injection with Eutasil (CEVA Santé Animale, France). *Tibialis anterior* muscle was isolated immediately, snap frozen in liquid N_2-cooled isopentane and stored at -80ºC for immunohistochemistry analysis.

1.5.2. pEGFP-NLS/BSA nanocapsules injection

To evaluate the *in vivo* transfection efficiency 300µL of the pEGFP-NLS/BSA nanocapsules (containing 20µg pEGFP-NLS) was intravenously injected once in tail vein of 4 mice. Two mice were injected with three hundred microliter of BSA nanocapsules solution (negative control). At 48h following injection, mice were sacrificed with Eutasil (CEVA Santé Animale, France). Liver and lungs were collected. A portion of each liver was collected, snap frozen in liquid N_2-cooled isopentane and stored at -80ºC for immunohistochemistry analysis. The remaining liver and the lungs were kept in PBS until being processed for flow cytometry analysis.

1.6. Flow cytometry analysis

Approximately $1x10^6$ transfected culture cells were washed with PBS, trypsinized and re-suspended in 1ml of DMEM supplemented with 10 % FBS. The supernatant was removed after centrifugation at 1000rpm for 5 minutes at

Eppendorf Centrifuge 5804 (Eppendorf) and cells were re-suspended in 500µL of DMEM supplemented with 10% FBS, in order to achieve approximately 2 million cells per millilitre for flow cytometry analysis.

The harvested mouse organ (liver or lungs) was pressed against a nylon mesh cell strainer of 70µm (Falcon, Ref. 352350) mounted on top of a 50mL Falcon tube and PBS was added to facilitate this process. The dispersed cells collected at the bottom of the tubes were diluted and centrifuged for 5 minutes at 1000 rpm on Eppendorf® Minispin® (Eppendorf).

Flow cytometry analysis was performed using FACSCalibur cytometer (BD Biosciences). About 300µl of cell suspension samples were analysed to detect GFP signal, using laser 488 and detector FL1 for *in vivo* and *in vitro* experiments. Signal acquisition was accessed using CellQuest™ software (BD Biosciences). A gate of 10 000 viable cells was selected. The quantification analysis was performed with FlowJo 8.7 Software (Tree Star, Inc. 1997-2012).

1.7. Fluorescent Immunohistochemistry

To access dystrophin expression, ten-micrometer thick transversal frozen sections of *tibialis anterior* from C57BL/6J wild type, m*dx52* negative control and *mdx52* treated mice with 10mg/kg LNA-AON were fixed with cold acetone for 10 minutes, permeabilized with 0.5% Triton X-100 on PBS, at room temperature for 10 minutes, incubated with blocking solution (1% BSA, 0.05% Tween 20) for 30 minutes in humid chamber, labelled with a rabbit polyclonal anti-dystrophin antibody (Abcam®, Cat. No. ab85302), diluted 1:100 in blocking solution, for 60 minutes and a secondary antibody anti-rabbit tetramethylrhodamine (TRITC) – conjugated affinity pure donkey (Jackson Imunoresearch Laboratories, Cat. No. 711-025-152), diluted 1:200 in blocking solution, for 60 minutes in humid chamber. The cellular nucleus was counterstained with DAPI (Sigma-Aldrich, Cat. No. D9542-5MG) with a final concentration of 1µg/ml, by 10 minutes incubation at RT. Coverslips were then mounted with antifade mounting medium (Vectashield, Vector Laboratories, Cat. No. H-1000).

To evaluate the transfection efficiency of pEGFP-NLS/BSA nanocapsules *in vivo,* ten-micrometer thick transversal frozen sections of liver from *mdx52* mice intravenously injected on tail vein with pEGFP-NLS/BSA nanocapsules (containing 20µg pEGFP-NLS) and 300µL of BSA nanocapsules solution (negative control) were fixed with 3.7% PFA on PBS for 10 minutes at room temperature, permeabilized with 0.5% Triton X-100 on PBS for 10 minutes, incubated with blocking solution (1% BSA, 0.05% Tween 20) for 30 minutes in humid chamber, labelled with a rabbit polyclonal anti-GFP antibody, Alexa Fluor® 488, (Termofisher, Cat. No. A-21311), diluted 1:200 in blocking solution, for 60 minutes and with a TRITC antirabbit secondary antibody (Jackson Imunoresearch Laboratories, Cat. No. 711-025-152), diluted 1:200 in blocking solution, for 60 minutes in humid chamber. The cellular nucleus was counterstained with DAPI (Sigma-Aldrich, Cat. No. D9542-5MG) with a final concentration of 1µg/ml, by 10 minutes incubation at RT. Coverslips were then mounted with antifade mounting medium (Vectashield, Vector Laboratories, Cat. No.H-1000).

1.8. Fluorescence Microscopy

Digital images from immunohistochemical analysis of dystrophin expression were captured using LEICA DM5000B Widefield Fluorescence Microscope (Leica Microsystems) with 40x dry objective (objective type: PL FLUOTAR), using Filterset Red (515-560nm) for dystrophin detection.

Cells grown on coverslips and transfected were fixed with 3.4% PFA (Paraformaldehyde) for 10 minutes RT, washed with PBS, mounted on slides and observed by fluorescence microscopy. Digital images from transfected HEK293 cells were captured using LEICA DM5000B Widefield Fluorescence Microscope (Leica Microsystems) with 40x dry objective (objective type: PL FLUOTAR), using Filterset blue (320-400nm) for DAPI detection and green (500-550nm) for GFP detection. This microscope has a monochrome CCD camera for fluorescence image acquisition and IrfanView as image acquisition software.

Digital images from immunohistochemistry analysis of GFP expression from *in vivo* experiments were captured using a Zeiss LSM 710 Confocal Point-Scanning Microscope (Carl Zeiss MicroImaging) with 400x magnification using the lasers Diode 405-30 for DAPI detection and DPSS 561-10 for GFP detection. Digital images were analysed with the software Image J and LSM 5 Image Browser (Zeiss).

Digital images of BSA nanoparticles encapsulating pEGFP-NLS were captured with 63x oil objective (model: Plan-Apochromat) using a Zeiss LSM 710 Confocal Point-Scanning Microscope (Carl Zeiss MicroImaging).

2. Results

2.1. LNA-AON to treat DMD in animal model

In our experiment, *mdx52* animals were intravenously injected once in tail vein with 10mg/kg of LNA-AON (treated) or saline solution (negative control). 11 weeks after injection, mice were euthanized and *tibialis anterior* muscle was collected. C57BL/6J mice muscles were also collected to be used as a positive control. Immunohistochemical staining of muscle cryosections was accessed and dystrophin production was evaluated through fluorescence microscopy.

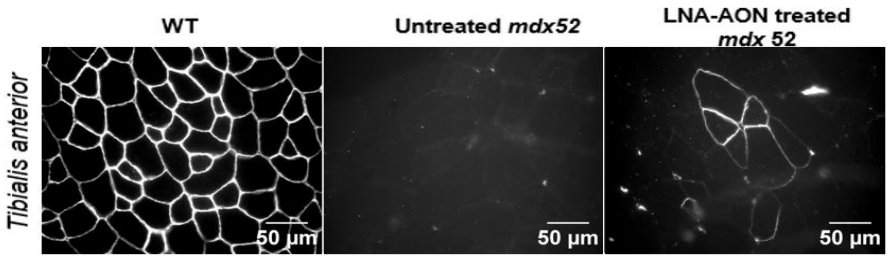

Figure 1 - **Immunohistochemical findings in *tibialis anterior*.** Dystrophin immunolabeling in muscle fibers. Representative fields of transversal sections from C57BL/6J wild type, untreated *mdx52* mice and LNA-AON (10mg/kg) treated *mdx52* mice, labelled with a rabbit polyclonal anti-dystrophin antibody, demonstrating absence of dystrophin in *mdx52* untreated mice and restoration of dystrophin in a group of muscles fibers after treatment with 10mg/kg of LNA-AON, 1 injection analysed 11 weeks after injection.

Immunohistochemistry of C57BL/6J mouse *tibialis anterior* muscle section revealed dystrophin protein localized at the sarcolemmal membrane of muscle fibers as expected, being used prospectively as our positive control. *Tibialis anterior* muscle section from untreated *mdx52* mouse dystrophic model do not show any dystrophin protein since the protein is completely absent in this mouse model. In *tibialis anterior* sections from LNA-AON treated *mdx52* mice, we could detect some muscle fibers with a positive stain for dystrophin protein. This results suggest a reversal of the phenotype for the production of DMD *in vivo* correctly localized at the sarcolemma. However when compared to *tibialis anterior* from C57BL/6J mouse model the number of corrected fibers is very low.

2.2. *In vitro* transfection of nucleic acids nanoparticles to establish analysis techniques

The low number of dystrophin positive fibers detected on muscle of LNA-AON treated animals shows that the exon skipping was achieved although it suggested that new delivery systems should be tested to improve delivery efficiency. Initially, the transfection efficiency of naked plasmid was accessed in Human Embryonic Kidney 293 (HEK293, ATCC® CRL-1573™).

HEK293 cells were transfected with two different amounts of pEGFP-NLS (0.013µg and 0.067µg). 48h after transfection the coverslips placed ate the bottom of each well were mounted and slides were observed under fluorescent microscopy. The quantification method of transfection efficiency was cell counting through merging of phase contrast and fluorescence images (Figure 2, A). A total of 641 cells were counted for transfection with 0.013µg plasmid, resulting in an average of 8.61 % GFP positive cells (S.D. 1.49). Concerning to cells transfected with 0.067µg of plasmid DNA, a total of 2944 cells were counted, resulting in an average of 14.21 % (S.D. 5,04) positive cells for GFP (Figure 2, B).

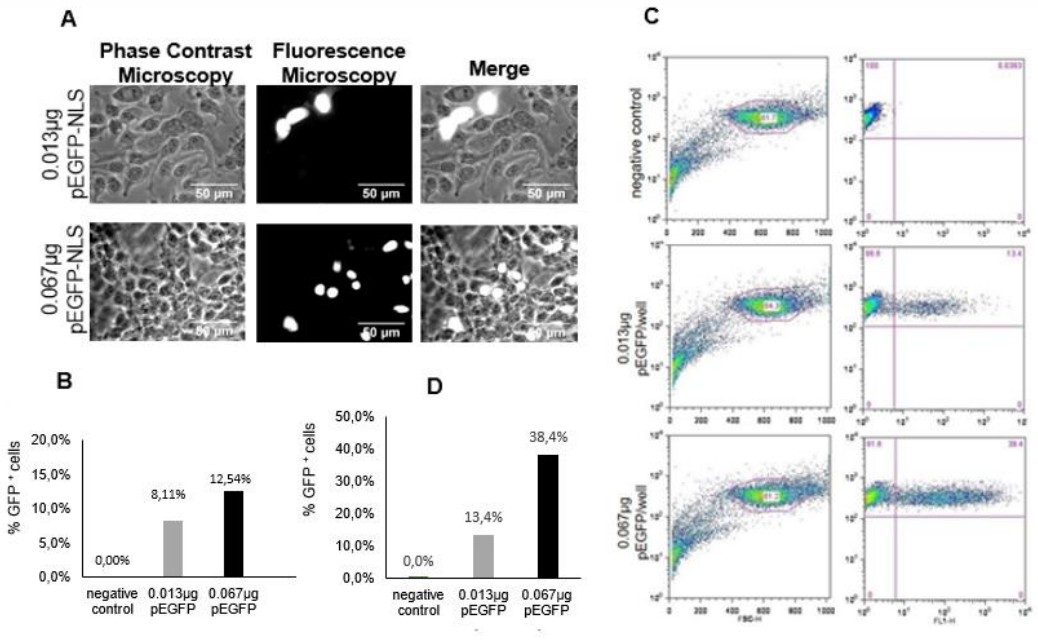

Figure 2 - Transfection efficiency on HEK 293 cells transfected with 0µg pEGFP-NLS/well, 0.013µg pEGFP-NLS/well and 0.067µg pEGFP-NLS/well. A – Fluorescence and phase contrast microscopy of the transfected HEK 293 cells as a 400x magnification; B– Results of microscopy analysis through cell counting (total of 2944 cells counted), C - Flow cytometry analysis using Cell Quest showing the % of viable cells and GFP positive cells; D - Results of flow cytometry analysis from FlowJo in approximately 10 000 detected events for each experiment.

In flow cytometry (Figure 2, C), 10 000 events were collected and analysed inside a gate of viable cells (set to every experiments) for each transfection experiment using Cell Quest. Data analysis was done with FlowJo software. In negative control, 61.2% of all events were considered as viable cells and GFP expression was then accessed inside that gate. As expected, no positive cells for GFP were found, consisting with results from fluorescence microscopy. For HEK293 cells transfected with 0.013µg and 0.067µg, the same gate was established, resulting in 63.9% and 60.8% of viable cells respectively. Concerning to GFP expression, results show that transfection was more efficiently for cells transfected with 0.067µg pEGFP-NLS (38.4 %), although transfection efficiency with 0.013µg pEGFP-NLS was also successfully achieved (13.4 %) (Figure 2, D). Thus, this experiment shows that a cell line is efficiently transfected by low concentrations of plasmid DNA, such as 0.013µg. The amount of pEGFP-NLS selected for the following experiments was 0.067µg.

Results obtained by fluorescent microscopy corresponds to results from flow cytometry, so, for the following experiments transfection efficiency was only evaluated by flow cytometry analysis.

Then, HEK293 cells were transfected with pEGFP-NLS encapsulated in BSA nanocapsules to set positive and negative controls before experiments *in vivo*. In the first experiment with nanocapsules, transfection efficiency of pEGFP-NLS/BSA nanocapsules were tested with and without Lipofectamine® 3000 (transfection agent). To compare efficiencies, cells were also transfected with naked plasmid with Lipofectamine® 3000. The results were analysed with fluorescent microscopy and flow cytometry.

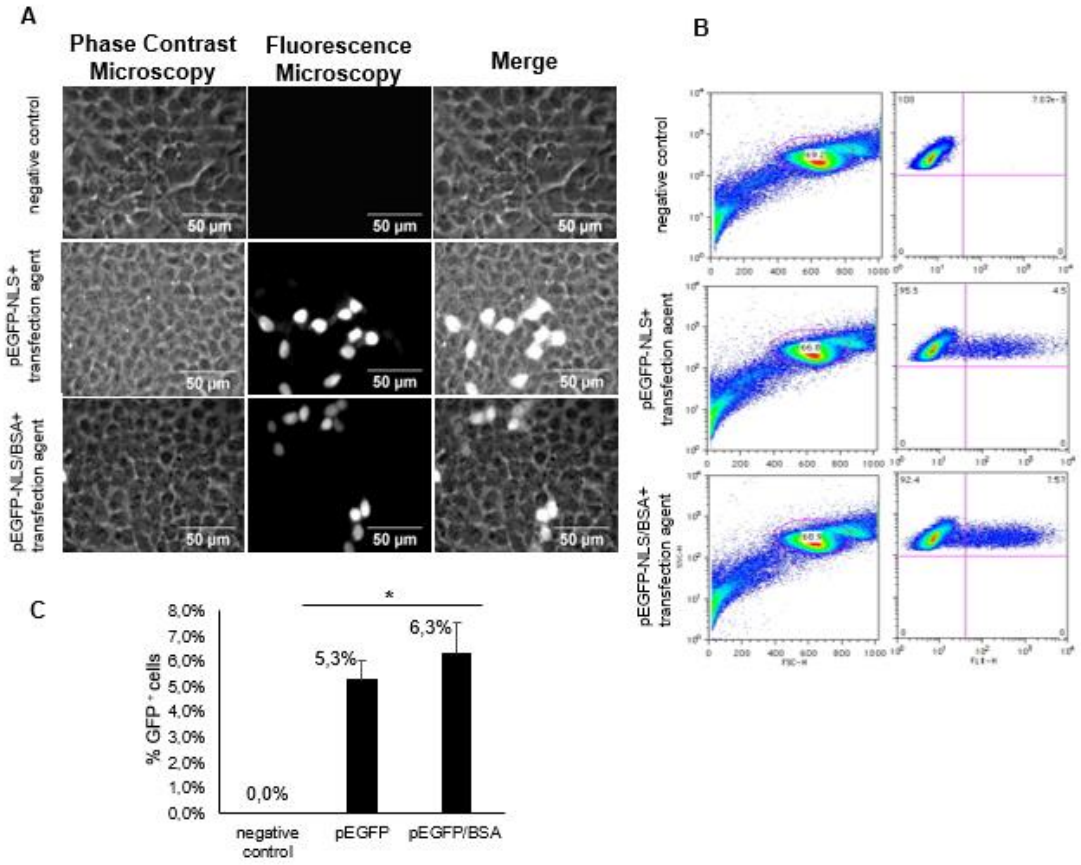

Figure 3 - Transfection efficiency on HEK 293 cells transfected with 0.067µg pEGFP-NLS per well, 0.067µg pEGFP-NLS/BSA per well, 0µg pEGFP-NLS/well with and without transfection agent. A – Fluorescence and phase contrast microscopy of the transfected HEK 293 cells as a 400x magnification; B– Flow cytometry analysis using Cell Quest showing the % of viable cells and GFP positive cells; C - Results of flow cytometry analysis from FlowJo in approximately 10 000 detected events for each experiment. *****: with transfection agent.

The fluorescent microscopy images suggest that transfection with naked pEGFP-NLS and pEGFP-NLS/BSA was correctly achieved *in vitro*. It is possible to see some fluorescent cells (positive cells for GFP) in both experiments using transfection agent (Lipofectamine® 3000). Transfection of BSA nanocapsules without Lipofectamine® 3000 had the same result as the negative control, once there were not found any positive cells (Figure 3, A). By flow cytometry analysis, the expression of GFP was analysed and quantified in approximately 10 000 viable cells for each experiment. In negative control, 69.2 % of all events were considered as viable cells and GFP expression was then quantified inside that gate. Consisting with microscope images, no fluorescent cells were detected. The 2 experiments using Lipofectamine® 3000 revealed rates of transfection very similar. An average of 5.28 % and 6.3 % of GFP positive cell for transfection with naked plasmid and with BSA nanocapsules, respectively (3 separated measures were done for each experiment) (Figure 3, B). To determine whether the difference between the rates of transfection with naked plasmid and nanocapsules, a statistical Kruskal-Wallis analysis with Dunn's multiple comparisons test was accessed with Graphpad. This test compared the means of 4 experiments and turns out that the difference between cells transfected with naked plasmid and with BSA nanocapsules is not significant (Figure 3, C).

A second experiment was performed to access transfection efficiently of naked plasmid without transfection agent in HEK293 cells. Images from fluorescence microscopy show a positive transfection for cells transfected with pEGFP-NLS/BSA nanocapsules helped with Lipofectamine® 3000. Both experiments without transfection agent, revealed no positive cells for GFP (Figure 4, A). Flow cytometry analysis confirms this results. From a selection of approximately 10 000 viable cells, an average of 10.2 % (S.D. 0.02) of GFP positive cells (Figure 4, C).

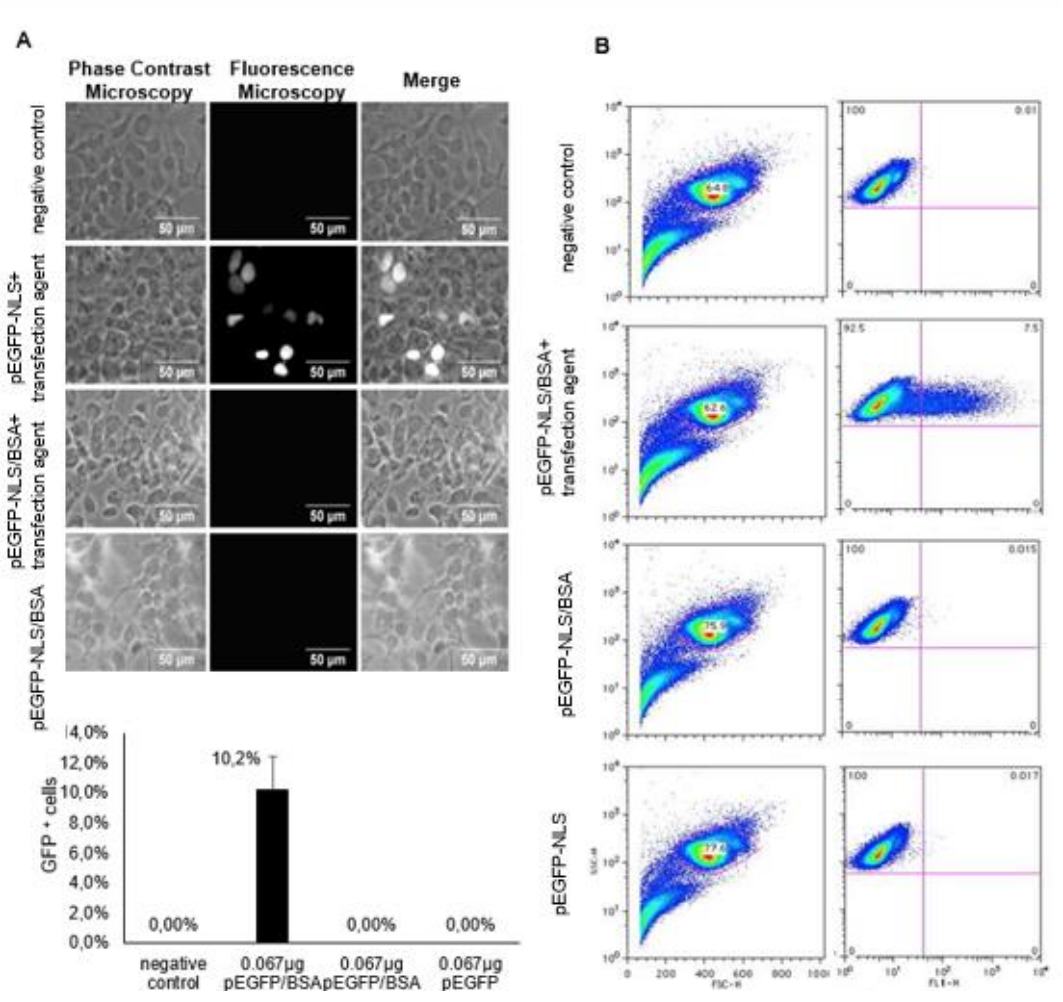

Figure 4 - Transfection efficiency on HEK 293 cells transfected with 0.067µg pEGFP-NLS/BSA per well with and without Lipofectamine® 3000, 0.067µg pEGFP-NLS per well without Lipofectamine® 3000 and 0µg pEGFP-NLS/well. A – Fluorescence and phase contrast microscopy of the transfected HEK 293 cells as a 400x magnification; B– Flow cytometry analysis using Cell Quest showing the % of viable cells and GFP$^+$ cells; C - Results of flow cytometry analysis from FlowJo in approximately 10 000 detected events for each experiment, resulting in an average of 10.2 % (S.D. 0.02) of GFP$^+$ cells.

The results in HEK293 cells shows that transfection was not efficiently when is absence of transfection agent, however results *in vitro* not always reflect results *in vivo*. So, we proposed to test transfection injection in *mdx52* mouse model.

2.3. *In vivo* injection

To evaluate the *in vivo* transfection efficiency 300µL of the pEGFP-NLS/BSA nanocapsules (containing 20µg pEGFP-NLS) was intravenously injected once in tail vein of 4 mice. Two mice were injected with three hundred microliter of empty BSA nanocapsules solution (negative control). At 48h following injection, mice were sacrificed with Eutasil (CEVA Santé Animale, France). Liver and lungs were collected. A portion of each liver was collected, snap frozen in liquid N_2-cooled isopentane and stored at -80ºC for immunohistochemistry analysis. The remaining liver and the lungs were kept in PBS until being processed for flow cytometry analysis.

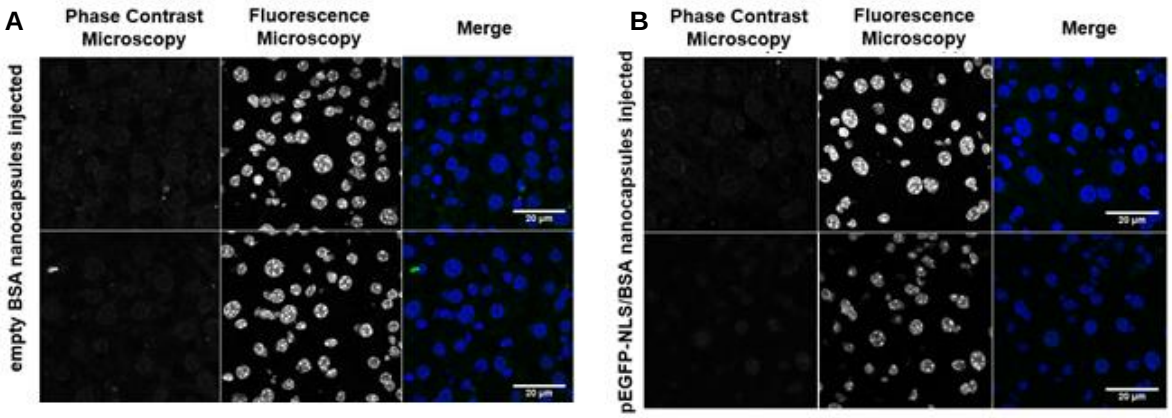

Figure 5 - **Immunohistochemical analysis by fluorescent microscopy of *in vivo* GFP gene expression by BSA nanoparticles loading EGFP pDNA. DAPI stained nucleus and GFP fluorescence are showed as blue and green, respectively in merge images.** (A) Digital images from liver of *mdx52* mouse model injected with empty BSA nanocapsules solution labelled with primary antibody anti-GFP Alexa 488, secondary antibody TRITC and nuclear staining DAPI. (B) Digital images from liver of *mdx52* mouse model injected with pEGFP-NLA/BSA solution labelled with primary antibody anti-GFP Alexa 488, secondary antibody TRITC and nuclear staining DAPI.

The plasmid selected to test *in vivo* transfection efficiency is a well-known genetic construct, pEGFP, and it was used as a reporter gene since it is fluorescent. This reporter gene has a NLS, so the fluorescent protein signal we see on microscope has a specific pattern. Frozen sections of liver from injected mice with empty BSA nanocapsules and with BSA nanocapsules encapsulating pEGFP were labelled with primary antibody anti-GFP Alexa 488, secondary antibody TRITC and DAPI for nuclear staining. Fluorescent microscopy images from animals injected with negative control solution (Figure 5, A) do not show positive cells for GFP in the green channel. Nuclear staining with DAPI was successfully achieved and so it is possible to see blue fluorescence for DAPI in the nuclei of liver cells. Merging images from green channel and DAPI shows that no GFP positive signal was found at cells nuclei. The same results were found for animals injected with pEGFP-NLS/BSA nanocapsules (Figure 5, B). We expected to see green signal inside cells nuclei, but merging images of green channel and DAPI suggests that pEGFP was not expressed, so we do not seen GFP positive signal inside cell nuclei.

Transfection efficiency of pEGFP-NLS/BSA nanocapsules in liver and lung of injected *mdx52* mouse model was also accessed by flow cytometry analysis.

48 hours after injection, isolated cells of liver and lung from mdx52 mouse model were collected and analysed by flow cytometry for GFP+ cells. The transfected cells were used as negative and positive controls to evaluate in vivo transfection efficiency (Figure 6, A). Concerning to liver of animals injected with empty BSA nanocapsules and animals injected with pEGFP-NLS/BSA nanocapsules (Figure 6, B), a gate of approximately 10 000 viable events were selected for both of them. Inside the defined gate no GFP fluorescence was detected by cytometer, as there are no significant differences between results for animals injected with empty BSA nanocapsules and animals injected with pEGFP-NLS/BSA nanocapsules. The same results were found in lung of animals injected with empty BSA nanocapsules and with pEGFP-NLS/BSA solution (Figure 6, C).

3.4. BSA nanocapsules stability assay

Based on results obtained *in vivo*, the stability of BSA nanocapsules was finally accessed by electrophoresis. 1µg of naked plasmid, pEGFP-NLS/BSA nanocapsules and BSA solution were run for 60 mins at 80V on 1 % agarose gel on TAE 1x buffer. As a positive control 1µg of naked plasmid was run in parallel. As a negative control also an equivalent amount of BSA empty nanoparticles. It can be seen from Figure 7 (A) that the pEGFP-NLS encapsulated in BSA nanocapsules is degraded once it does not show a perfect band as the naked plasmid but most of the observed

DNA has a smeared pattern. The BSA nanocapsules does not reveals a band as expected from a negative control. We hypothesised that pDNA encapsulation could be changing the pattern of migration and that the smeared pattern could be due to the fact of pDNA be encapsulated. Thus, we assumed that by digestion of the proteic capsule the released pDNA would show a migration pattern similar to the one of the naked plasmid DNA. Naked plasmid DNA was also digested with proteinase K as a control for pDNA degradation in this assay (Figure 7, B).

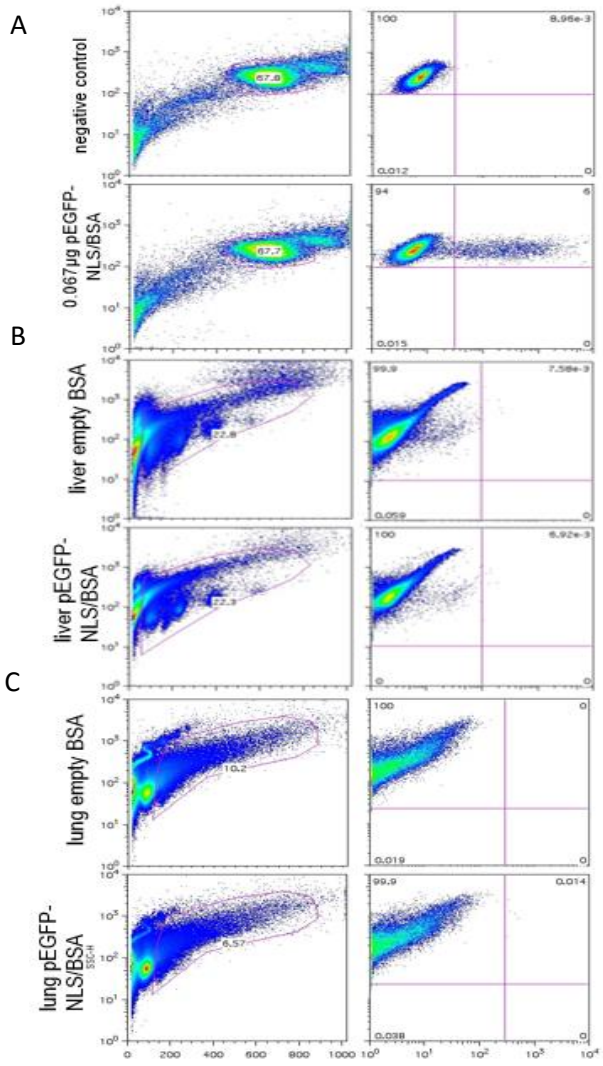

Figure 6 - **Flow cytometry analysis using acquired with Cell Quest showing the % of viable cells and GFP positive cells in approximately 10 000 events**; (A) Transfected HEK293 cells as negative and positive control; (B) Results in liver of *mdx52* mouse model injected with empty BSA nanocapsules solution and with pEGFP-NLS/BSA solution were both approximately 0.00%; (C) Results in lung of *mdx52* mouse model injected with empty BSA nanocapsules solution and with pEGFP-NLS/BSA solution were both approximately 0.00%.

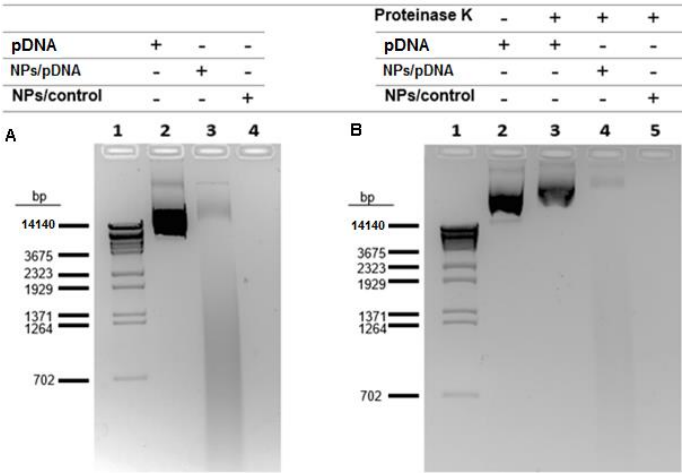

Figure 7 - Agarose gel electrophoresis results of naked plasmid DNA, pEGFP-NLS/BSA nanocapsules and BSA nanocapsules solution after (A) and following Proteinase K digestion (B). Samples were run on a 1 % gel for 60 minutes at 80 V.

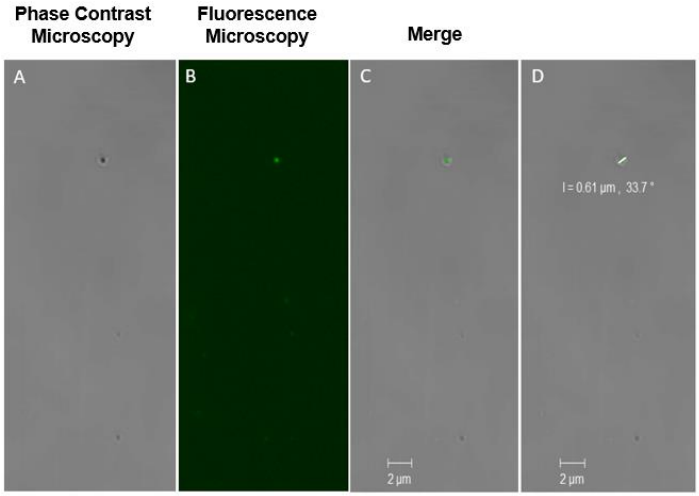

Figure 8 - Encapsulated pDNA on BSA nanoparticles can be visualized by fluorescence microscopy. pEGFP-NLS/BSA nanocapsules were stained with Coomassie blue and with Hoechst 33342 for protein and nucleic acid stain, respectively, and imaged on the confocal fluorescence microscope. The protein capsule can be seen on the phase contrast image overlapping with a blue fluorescent signal from Hoechst that is here intentionally depicted in green to better visualization on the image. The same field is illustrated in (A) Phase-contrast; (B) fluorescence and (C) merging of former images.

The result obtained for the analysis of the pEGFP-NLS/BSA nanocapsules is the same as in the previous assay, confirming that the smeared pattern was due to pDNA degradation.

Images of nanoparticles highlighted by Hoechst 33342 were also obtained through fluorescence confocal microscopy. Hoechst 33342 nucleic acid stain is a popular cell-permeant nuclear counterstain that emits blue fluorescence when bound to double-stranded DNA (dsDNA). It was possible to see the proteic nanoparticle in phase-contrast (Figure 18, A) overlapping with the fluorescent signal of the nucleic acid stain (Figure 18, B and C). The size of visualized nanoparticles is variable but less than 1µm (Figure 18, D).

4. Discussion

In this study we proposed using bovine serum albumin (BSA) nanoparticles as a vehicle to *in vivo* delivery of nucleic acids. As a reporter we chose a DNA construct, a plasmid coding for GFP containing an NLS, in order to access the functional uptake of the encapsulated nucleic acid to tissue cells in a mouse model. It is described in literature that a

target organ for DNA systemic delivery is the liver (e.g. Rimessi et al, 2009; Tomoaki K. et al, 2011) and also the lungs (Tomoaki K. et al, 2011; Kodama Y., et al, 2014) and we chose those organs to evaluate the uptake and effective expression of our reporter plasmid. In order to quantitatively evaluate transfected cells in mouse liver and lungs a flow cytometry method was chosen (Caiado et al, 2013). To evaluate correct localization and patterns of GFP fluorescence in tissues a fluorescence histochemical method was elected.

HEK293 cells transfected with pEGFP-NLS/BSA nanoparticles were analysed through fluorescent microscopy and flow cytometry to evaluate transfection efficiency. We also would expect an efficient *in vitro* transfection of HEK293 cells only by adding DNA loaded-nanoparticles without any transfection agent based on published papers that show successful transfection experiments with nanoparticles loading pDNA *in vitro*. However, in our experiment, fluorescent microscopy and flow cytometry analysis of HEK293 cells transfect with pEGFP-NLS/BSA nanocapsules revealed that transfection and GFP expression was not achieved. Despite this results, we proposed to test transfection efficiency *in vivo* once results obtained *in vitro* do not always reflect results *in vivo.*

Transfection efficiency was evaluated in liver and lung of injected animals through immunohistochemical analysis with specific antibodies targeting GFP protein and by flow cytometry. Experiments with injected animals with pEGFP-NLS/BSA nanocapsules solution did not resulted in satisfactory transfection rates neither by fluorescent microscopy or flow cytometry analysis. Based on this results, we proposed to evaluate our nanoparticles through electrophoresis and results suggests that pDNA encapsulated in BSA nanoparticles was degraded as it shows a smeared band instead of a perfect one in images of gel documentation.

Some possible reasons for results obtained *in vitro* and *in vivo* might be related with lack of a complete characterization of BSA nanoparticles used in this experiment for example in terms of ability to protect plasmid DNA from degradation. The concentration of pDNA encapsulated on nanoparticles should also have been confirmed.

It will be interesting to repeat the experiments in a more controlled way, however we suggest that the methodologies used are correct. Future investigations should invest in nanocapsules directed target to increase the efficiency delivery of nucleic acids. Nanomaterials are certainly very appealing as nucleic acids vehicles and show great promise in this regard.

5. Conclusions and Future Perspectives

Drug delivery is certainly a key factor in the optimization of treatment efficacy and efficiency, and may enable us to reduce undesirable off-target effects, side effects, and the dose requirement. Significant progress has been made4 during the recent years in nanoscale drugs and delivery systems employing diverse chemical formulations to facilitate the rate of drug delivery and improve its pharmacokinetics. Biocompatible nanomaterials have been manly used as drug delivery systems. Concerning to Duchenne Muscular Dystrophy, antisense oligonucleotides (AONs) have shown promising results. However, delivery to target tissue (striated muscle) has proved challenging.

Continuous advances in synthetic chemistry and material chemistry will help realizing such novel classes of nanoparticles and nanoscale systems with integrated functionalities and properties. For example, multifunctional nanoparticles probes are recently being developed to overcome limitation inherent in single component platforms such as multimodal contrast agents comprised of magnetic nanoparticles coupled with either optical or radiolabelled probes that allow medical imaging in two modes. In fact, Qian and colleagues developed this year, a biodegradable double nanocapsule, made of BSA and PLGA, as a novel multifunctional carrier for drug delivery and cell imaging. Therefore, such a multifunctional capsules system could be considered as a new promising methodology for targeting and treating diseases like cancer (Qian et al, 2015).

6. References

Aoki Y, Nakamura A, Yokota T, Saito T, Okazawa H, Nagata T, Takeda S, “In-frame dystrophin following exon 51-skipping improves muscle pathology and function in the exon 52-deficient *mdx* mouse,” *Molecular Therapy*, vol. 18, no. 11, pp. 1995–2005, 2010

Elsadek B, Kratz F, “Impact of albumin on drug delivery – New applications on the horizon”, *Journal of Controlled Release,* Vol. 157, pp. 4–28, 2011.

Falzarano M, Passarelli C, Ferlini A, “Nanoparticle Delivery of Antisense Oligonucleotides and Their Application in the Exon Skipping Strategy for Duchenne Muscular Dystrophy”, *Nucleic Acid Therapeutics”*, Vol. 24, No. 1, 2014.

Qian K, Wu J, Zhang E, Zhang Y, Fu A, “Biodegradable double nanocapsules as a novel multifunctional carrier for drug delivery and cell imaging”, *International Journal of Nanomedicine*, Vol. 10, pp. 4149–4157, 2015.

Shimanovich U, Bernardes G, Knowles TPJ, Cavaco-Paulo A, “Protein micro- and nano-capsules for biomedical applications”, *The Royal Society of Chemistry*, Vol. 43, pp. 1361–1371, 2014Wein et al, “Genetics and Emerging Treatments for Duchenne and Becker Muscular Dystrophy”, *Pediatr. Clin. N. Am.*, 2015